CellPress

Cancer Cell
Article

A Long Noncoding RNA Activated by TGF-β Promotes the Invasion-Metastasis Cascade in Hepatocellular Carcinoma

Ji-hang Yuan,[1] Fu Yang,[1] Fang Wang,[1] Jin-zhao Ma,[1] Ying-jun Guo,[1] Qi-fei Tao,[2] Feng Liu,[1] Wei Pan,[1] Tian-tian Wang,[1] Chuan-chuan Zhou,[1] Shao-bing Wang,[1] Yu-zhao Wang,[1] Yuan Yang,[2] Ning Yang,[3] Wei-ping Zhou,[2] Guang-shun Yang,[3] and Shu-han Sun[1,*]

[1]Department of Medical Genetics, Second Military Medical University, Shanghai, 200433, China
[2]The Third Department of Hepatic Surgery, Eastern Hepatobiliary Hospital, Second Military Medical University, Shanghai, 200433, China
[3]The Fifth Department of Hepatic Surgery, Eastern Hepatobiliary Hospital, Second Military Medical University, Shanghai, 200433, China
*Correspondence: shsun@vip.sina.com
http://dx.doi.org/10.1016/j.ccr.2014.03.010

SUMMARY

The role of TGF-β-induced epithelial-mesenchymal transition (EMT) in cancer cell dissemination is well established, but the involvement of lncRNAs in TGF-β signaling is still unknown. In this study, we observed that the lncRNA-activated by TGF-β (lncRNA-ATB) was upregulated in hepatocellular carcinoma (HCC) metastases and associated with poor prognosis. lncRNA-ATB upregulated ZEB1 and ZEB2 by competitively binding the miR-200 family and then induced EMT and invasion. In addition, lncRNA-ATB promoted organ colonization of disseminated tumor cells by binding IL-11 mRNA, autocrine induction of IL-11, and triggering STAT3 signaling. Globally, lncRNA-ATB promotes the invasion-metastasis cascade. Thus, these findings suggest that lncRNA-ATB, a mediator of TGF-β signaling, could predispose HCC patients to metastases and may serve as a potential target for antimetastatic therapies.

INTRODUCTION

Hepatocellular carcinoma (HCC) is one of the most common and aggressive human malignancies in the world (Jemal et al., 2011). The poor prognosis and high recurrence rate of HCC is largely due to the high rate of intrahepatic and extrahepatic metastases (Budhu et al., 2006). This emphasizes the urgency of identifying these patients in advance and establishing new therapeutic targets for successful intervention. Metastasis is a complex process, and many cell-intrinsic identities and extrinsic microenvironment factors influence the metastatic potential of HCC cells (Fidler, 2003). However, the underlying molecular mechanisms that mediate the metastatic cascade remain largely unclear. Enhancing our understanding of the molecular mechanisms may promote the development of effective metastasis-targeted therapy and improve the overall prognosis of patients with HCC.

The multifunctional cytokine transforming growth factor β (TGF-β) orchestrates an intricate signaling network to modulate tumorigenesis and progression (Majumdar et al., 2012; Massagué, 2008). TGF-β exerts its tumor-suppressive role by inducing cell-cycle arrest and apoptosis (Pardali and Moustakas, 2007). Nevertheless, TGF-β also promotes tumor progression through enhancing proliferation, migration, and invasion, in part by its ability to induce epithelial-mesenchymal transition (EMT) (Akhurst and Hata, 2012). EMT has been shown to be of critical importance in the early events of tumor cell metastatic dissemination by endowing cells with a more motile, invasive potential (Thiery et al., 2009). However, the involvement of EMT and its reverse process, mesenchymal-epithelial transition (MET) in the late events of tumor cell metastasis, such as distant colonization, are still hotly debated (Ocaña et al., 2012; Tsai et al., 2012). The multiple and often contradictory functions of TGF-β necessitate both a better understanding of the special downstream effectors

Significance

Metastases account for the vast majority of cancer-associated deaths and TGF-β-induced EMT has been associated with tumor invasion. However, the tumor-suppressive role of TGF-β hinders the application of anti-TGF-β cancer treatments. The involvement of EMT in metastatic colonization is still hotly debated. We found that lncRNA activated by TGF-β (lncRNA-ATB) can mimic the prometastatic role of TGF-β. lncRNA-ATB induced EMT and tumor cell invasion and promoted the colonization of disseminated tumor cells. High expression of lncRNA-ATB is a robust predictor of poor survival. Therefore, lncRNA-ATB may serve as a target for therapeutic intervention against cancer metastases early in the metastatic process and when patients present with circulating tumor cells.

of TGF-β and a search for specific inhibitors of the different TGF-β-dependent pathways for HCC treatment.

Long noncoding RNAs (lncRNAs) are a class of transcripts longer than 200 nucleotides with limited protein coding potential. Recently, many studies have shown that lncRNAs are frequently deregulated in various diseases and have multiple functions in a wide range of biological processes, such as proliferation, apoptosis, or cell migration (Mercer et al., 2009; Ponting et al., 2009). Although several lncRNAs have been reported to modulate tumor metastases (Gupta et al., 2010; Prensner et al., 2013), the specific roles of lncRNAs in mediating the prometastatic role of TGF-β and regulating EMT are not well studied. In this study, we report the identification of lncRNA-AL589182.3 (ENST00000493038), which we have named lncRNA-activated by TGF-β (lncRNA-ATB), and focus on the role of lncRNA-ATB in TGF-β signaling and in the invasion-metastasis cascade of HCC.

RESULTS

lncRNA-ATB Is Upregulated by TGF-β and Is Physically Associated with the miR-200 Family

To identify lncRNAs that are regulated by TGF-β and mediated the role of TGF-β in inducing EMT, we treated SMMC-7721 hepatoma cells continuously with TGF-β for 21 days, which caused SMMC-7721 cells to undergo EMT, as indicated by a spindle-shaped appearance (Figure S1A available online), decreased expression of the epithelial marker CDH1, and increased expression of the mesenchymal markers and transcription factors CDH2, VIM, ZEB1, SNAI1, and TWIST1 (Figure S1B). We then used microarray analysis to compare lncRNA expression levels between TGF-β treated and untreated cells, and found 676 upregulated and 297 downregulated lncRNAs in the treated cells (Table S1). Microarray results also indicated that TGF-β treatment led to EMT gene expression signature (Figure S1C; Huang et al., 2012) and gene set enrichment analysis (GSEA; Subramanian et al., 2005) indicated that four published TGF-β response signatures (Calon et al., 2012; Kang et al., 2003; Padua et al., 2008) were significantly enriched in the treated cells (Figure S1D), which further confirmed that the microarray results were trustable and TGF-β treatment for 21 days indeed induced EMT.

Recently, many RNA transcripts have been reported to function as competing endogenous RNAs (ceRNA) by competitively binding common microRNAs (Cesana et al., 2011; Salmena et al., 2011; Tay et al., 2011). The miR-200 family, including miR-200a, miR-200b, miR-200c, miR-141, and miR-429, has been reported to repress EMT and tumor invasion by targeting the 3′UTRs of ZEB1 and ZEB2 (Burk et al., 2008; Gregory et al., 2008). Among the deregulated lncRNAs, we predicted 76 miR-200s targeting sites on 46 lncRNAs (Table S2) using the TargetScan prediction algorithm (Lewis et al., 2005; http://www.targetscan.org/). Interestingly, one of the upregulated lncRNAs, lncRNA-ATB, which has a relatively large fold change, has three predicted miR-200s targeting sites in a relatively short span (Figures 1A and 1B), indicating a strong possibility as a ceRNA (Tay et al., 2011).

To confirm the microarray result, we treated SMMC-7721 and the normal liver cell line QSG-7701 with TGF-β and measured the expression of lncRNA-ATB at various time points. TGF-β induced a robust increase of lncRNA-ATB in both cells, not only in the long-term treatment, but also in short-term treatment (Figures 1C–1F). In breast cancer cell line MCF7 and colorectal cancer cell line SW480, TGF-β also upregulated lncRNA-ATB (Figures S1E and S1F).

The sequence of full-length lncRNA-ATB is presented in Figures S1G and S1H. Northern blot analysis of lncRNA-ATB confirmed the expected size (Figure 1G). Using a BLAST search of the sequence of lncRNA-ATB against the human genome, we found another three highly homologous lncRNA-ATB loci on chromosomes 13, 14, and 22, suggesting there may be an lncRNA family, which includes lncRNA-ATB. lncRNA-ATB was poly (A)-negative and mainly located in the cytoplasm (Figures S1I and S1J). Analysis of the sequences by ORF Finder from the National Center for Biotechnology Information failed to predict a protein of more than 55 amino acids (Figure S1K). Moreover, lncRNA-ATB does not contain a valid Kozak sequence. In addition, we used txCdsPredict from UCSC and PhyloCSF (Lin et al., 2011) to calculate its coding potential. The txCdsPredict score of lncRNA-ATB is 309.5 and the codon substitution frequency score is lower than −500 (Figure S1L), which further supports that lncRNA-ATB has no protein-coding potential. An analysis with quantitative (q)RT-PCR revealed a significantly higher expression of lncRNA-ATB in HCC cells than in normal liver cells, especially in highly metastatic cells (Figures S1M and S1N).

To validate the direct binding between miR-200s and lncRNA-ATB at endogenous levels, we performed an RNA immunoprecipitation (RIP) to pull down endogenous microRNAs associated with lncRNA-ATB and demonstrated via qPCR analysis that the lncRNA-ATB RIP in SMMC-7721 cells was significantly enriched for miR-200s compared to the empty vector (MS2), IgG, nontargeting microRNA (miR-122), lncRNA-ATB with mutations in miR-200s targeting sites (henceforth named ATB-mut(miR-200)), and another lncRNA-ENST00000508851 (RP11-893F2.9; henceforth named lncRNA-508851), which is also induced by TGF-β, but does not have a predicated miR-200s targeting site (Figure 1H; Figure S1O). The specific association between miR-200s and lncRNA-ATB was further validated by affinity pull-down of endogenous miR-200s using in vitro transcribed biotin-labeled lncRNA-ATB (Figure 1I). For further confirmation, we constructed luciferase reporters containing the 3′ 500nt of lncRNA-ATB, which contains wild-type (WT) or mutated miR-200s binding sites. We found that overexpression of miR-200s reduced the luciferase activities of the WT reporter vector but not empty vector or mutant reporter vector (Figure 1J). However, we found no significant difference in lncRNA-ATB levels after overexpression of miR-200s (Figure S1P). The microRNAs are known to bind their targets and cause translational repression and/or RNA degradation in an AGO2-dependent manner. To determine whether lncRNA-ATB was regulated by miR-200s in such a manner, we conducted anti-AGO2 RIP in SMMC-7721 cells transiently overexpressing miR-200s. Endogenous lncRNA-ATB pull-down by AGO2 was specifically enriched in miR-200s-transfected cells (Figure 1K), supporting that miR-200s are bona fide lncRNA-ATB-targeting microRNAs. These data demonstrated that miR-200s bound to lncRNA-ATB but did not induce the degradation of lncRNA-ATB. Ectopically expressed lncRNA-ATB WT, but not the mutant or lncRNA-508851, reduced the levels of miR-200s (Figure S1Q). To function

A

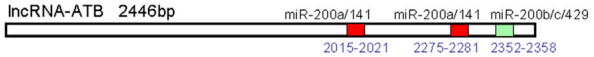

B

microRNA	matching	position
miR-200a	3' uguAGCAAUGGU- -CUGUCACAAu 5' 5' aacT TGTAGCCACCTTCAGTGTTt 3'	2015-2021
miR-141	3' ggUAGAA- AU- GGU- -CUGUCACAAu 5' 5' atAACTTGTAGCCACCTTCAGTGTTt 3'	2015-2021
miR-200a	3' uguagcaaugguCUGUCACAAu 5' 5' ga ta tccag t t tGACAGTGTTc 3'	2275-2281
miR-141	3' ggUAGAAAU-GGUCUGUCACAAu 5' 5' ggATATCCAGTT TGACAGTGTTc 3'	2275-2281
miR-200b	3' aguaguaaugguccgUCAUAAU 5' 5' aacagagaguaacagAGUAUUA 3'	2352-2358
miR-200c	3' agguaguaaugggccgUCAUAAU 5' 5' caacagagaguaacagAGUAUUA 3'	2352-2358
miR-429	3' ugccaaaauggucugUCAUAAU 5' 5' aacagagaguaacagAGUAUUA 3'	2352-2358

C

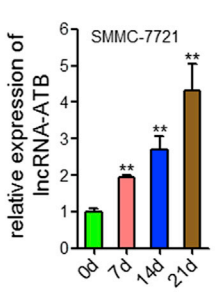

D

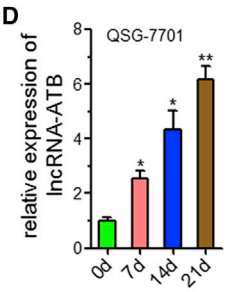

E

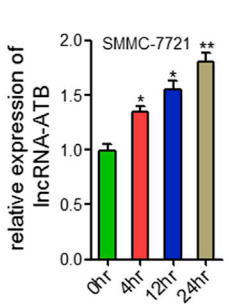

F

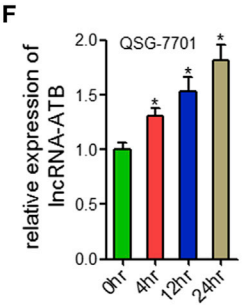

G

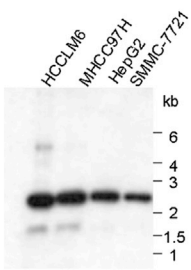

H

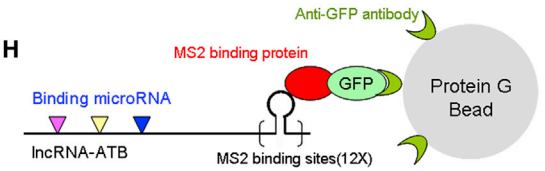

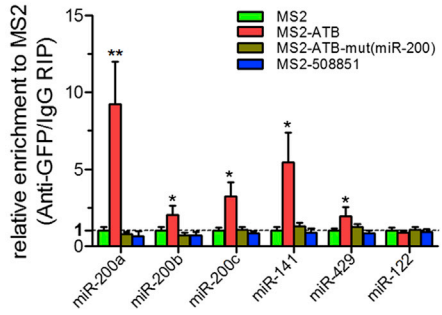

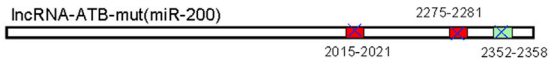

I

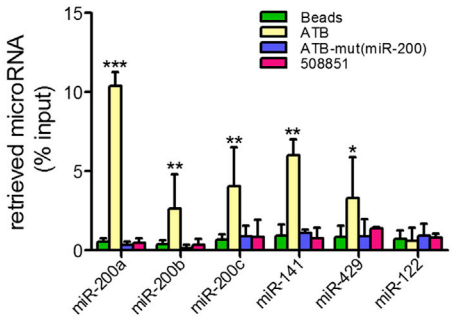

J

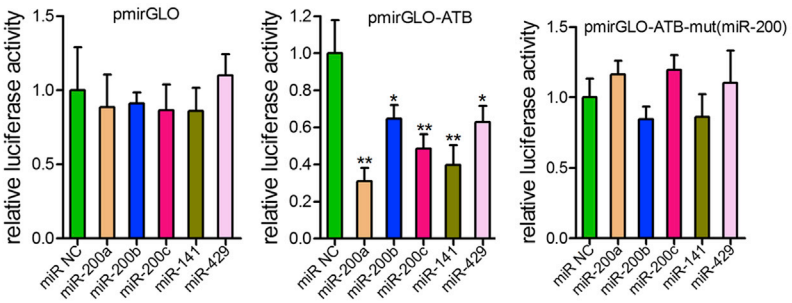

K

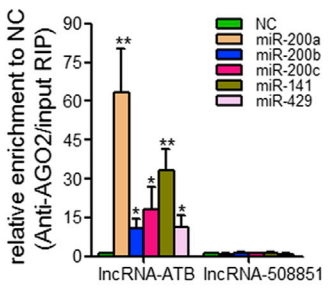

(legend on next page)

as a ceRNA, the abundance of lncRNA-ATB and miR-200s should be comparable. We therefore used quantitative real-time PCR to quantify the exact copy numbers of lncRNA-ATB and miR-200s per cell in TGF-β treated and untreated SMMC-7721 cells. We formulated standard curves with limit dilution approaches using lncRNA-ATB expressing vector pcDNA3.1-ATB and reverse-transcribed miR-200s cDNA as standard templates, and then the exact copy numbers of lncRNA-ATB and miR-200s per cell were calculated according to cell counts and molecular weights. As a result, we found that in the untreated cells, the expression level of lncRNA-ATB was approximately 100 copies per cell, and mature miR-200s levels were approximately 200 copies per cell. TGF-β treatment induced upregulation of lncRNA-ATB and downregulation of miR-200s (Figure S1R). This result implied that lncRNA-ATB may be able to function as a ceRNA for miR-200s. All these data demonstrated that lncRNA-ATB physically associated with the miR-200 family and may function as a ceRNA.

lncRNA-ATB Upregulates ZEB1 and ZEB2 Levels

Because lncRNA-ATB shares regulatory miR-200s with ZEB1 and ZEB2, we wondered whether lncRNA-ATB could modulate ZEB1 and ZEB2 and then EMT and invasion of HCC cells. We stably overexpressed lncRNA-ATB WT, lncRNA-ATB-mut(miR-200), and lncRNA-508851 in SMMC-7721 cells (Figure 2A; Figure S2A). The overexpression level of mutant clone is similar to that of WT overexpression clone 1, which is also comparable to that in highly metastatic HCCLM6 cells. For the rescue experiment, we stably overexpressed miR-200a in lncRNA-ATB overexpression clone 1 (Figure S2B). Overexpression of lncRNA-ATB WT, but not the mutant or lncRNA-508851, increased ZEB1 and ZEB2 transcript and protein levels in a dose-dependent manner. Ectopic expression of miR-200a abrogated this increase (Figures 2B and 2C). In QSG-7701 cells, stable overexpression of lncRNA-ATB also upregulated ZEB1 and ZEB2 (Figures 2D–2F). Additionally, HCCLM6 cells with stably downregulated lncRNA-ATB or lncRNA-508851 were also constructed, which do not have any effect on other family members of lncRNA-ATB (Figure 2G; Figures S2C and S2D). For the rescue experiment, we inhibited miR-200a in lncRNA-ATB downregulated HCCLM6 clone 1 (Figure S2E). The depletion of lncRNA-ATB, but not lncRNA-508851, decreased ZEB1 and ZEB2 in a dose-dependent manner. Inhibition of miR-200a overcame the decrease of ZEB1 and ZEB2 (Figures 2H and 2I).

To ascertain whether this observed effect depends on regulation of the ZEB1 and ZEB2 3′UTR, we constructed luciferase reporters containing either the ZEB1 or ZEB2 3′UTR (pmirGLO-ZEB1 or pmirGLO-ZEB2). Luciferase plasmid (pmirGLO-ZEB1, pmirGLO-ZEB2, or the control reporter [pmirGLO]) was transfected into the different SMMC-7721 and HCCLM6 cell clones. Overexpression of lncRNA-ATB, but not the mutant or lncRNA-508851, increased the luciferase activity of pmirGLO-ZEB1 and pmirGLO-ZEB2 in a dose-dependent manner. Ectopic expression of miR-200a abolished this upregulation (Figure 2J). Reciprocally, the depletion of lncRNA-ATB, but not lncRNA-508851, decreased the luciferase activity of pmirGLO-ZEB1 and pmirGLO-ZEB2, which were rescued by inhibition of miR-200a (Figure 2K).

Because lncRNA-ATB could upregulate ZEB1 and ZEB2, we next examined whether lncRNA-ATB is coexpressed with ZEB1 and ZEB2 in human HCC samples. We measured the expression levels of lncRNA-ATB, ZEB1, and ZEB2 in 86 human HCC tissues. As shown in Figures 2L and 2M, lncRNA-ATB transcript level was significantly correlated with ZEB1 or ZEB2 mRNA level. All these results suggest an important role of lncRNA-ATB in modulating ZEB1 and ZEB2 by competitively binding miR-200s.

lncRNA-ATB Induces EMT and Cell Invasion In Vitro

To investigate whether lncRNA-ATB regulates EMT through modulating ZEB1 and ZEB2, we first examined the effect of lncRNA-ATB on cell phenotypes. Overexpression of lncRNA-ATB WT, but not the mutant or lncRNA-508851, induced mesenchymal-like morphological feature in SMMC-7721 cells. Ectopic expression of miR-200a caused lncRNA-ATB overexpressed cells to revert to an epithelial phenotype (Figure 3A). Analysis of the epithelial markers E-cadherin and ZO-1 and the mesenchymal markers N-cadherin and vimentin revealed that overexpression of lncRNA-ATB, but not the mutant or lncRNA-508851, reduced E-cadherin and ZO-1 and increased N-cadherin and vimentin. Consistently, ectopic expression of miR-200a abolished the effects (Figures 3B and 3C). Immunofluorescence staining also revealed that overexpression of lncRNA-ATB, but not the mutant or lncRNA-508851, induced loss of E-cadherin and ZO-1 expression from the cell membrane, and increased N-cadherin and vimentin, which was also abolished by overexpression of miR-200a (Figure 3D). Conversely, the depletion of lncRNA-ATB, but not lncRNA-508851, induced an epithelial phenotype, upregulated E-cadherin and ZO-1, as well as downregulated N-cadherin and vimentin in HCCLM6 cells, which were also abrogated by inhibition of miR-200a (Figures 3E–3G). Moreover, depletion of lncRNA-ATB attenuated TGF-β-induced EMT in SMMC-7721 cells (Figure S3A; Figures 3H and 3I). Overexpression of lncRNA-ATB also induced EMT in QSG-7701 cells and MCF7 cells (Figures S3B–S3H). To further support this conclusion, we construct stable SMMC-7721 cell clone that overexpressed

Figure 1. lncRNA-ATB Is Upregulated by TGF-β and Interacts with miR-200s

(A) Schematic outlining the predicted binding sites of miR-200s on lncRNA-ATB.

(B) The prediction for miR-200s binding sites on lncRNA-ATB transcript. The red nucleotides are the seed sequences of microRNAs.

(C–F) Relative expression of lncRNA-ATB in SMMC-7721 cells or QSG-7701 cells treated with TGF-β1 for the indicated time was measured by qRT-PCR.

(G) Northern blot analysis of lncRNA-ATB in HCC cells.

(H) MS2-RIP followed by microRNA qRT-PCR to detect microRNAs endogenously associated with lncRNA-ATB.

(I) SMMC-7721 cell lysates were incubated with biotin-labeled lncRNA-ATB; after pull-down, microRNAs was extracted and assessed by qRT-PCR.

(J) Luciferase activity in SMMC-7721 cells cotransfected with miR-200s and luciferase reporters containing nothing, lncRNA-ATB or mutant transcript. Data are presented as the relative ratio of firefly luciferase activity to renilla luciferase activity.

(K) Anti-AGO2 RIP was performed in SMMC-7721 cells transiently overexpressing miR-200s, followed by qRT-PCR to detect lncRNA-ATB or lncRNA-508851 associated with AGO2.

Data are shown as mean ± SD; n = 3. *$p < 0.05$, **$p < 0.01$, ***$p < 0.001$ (Student's t test). See also Figure S1 and Tables S1 and S2.

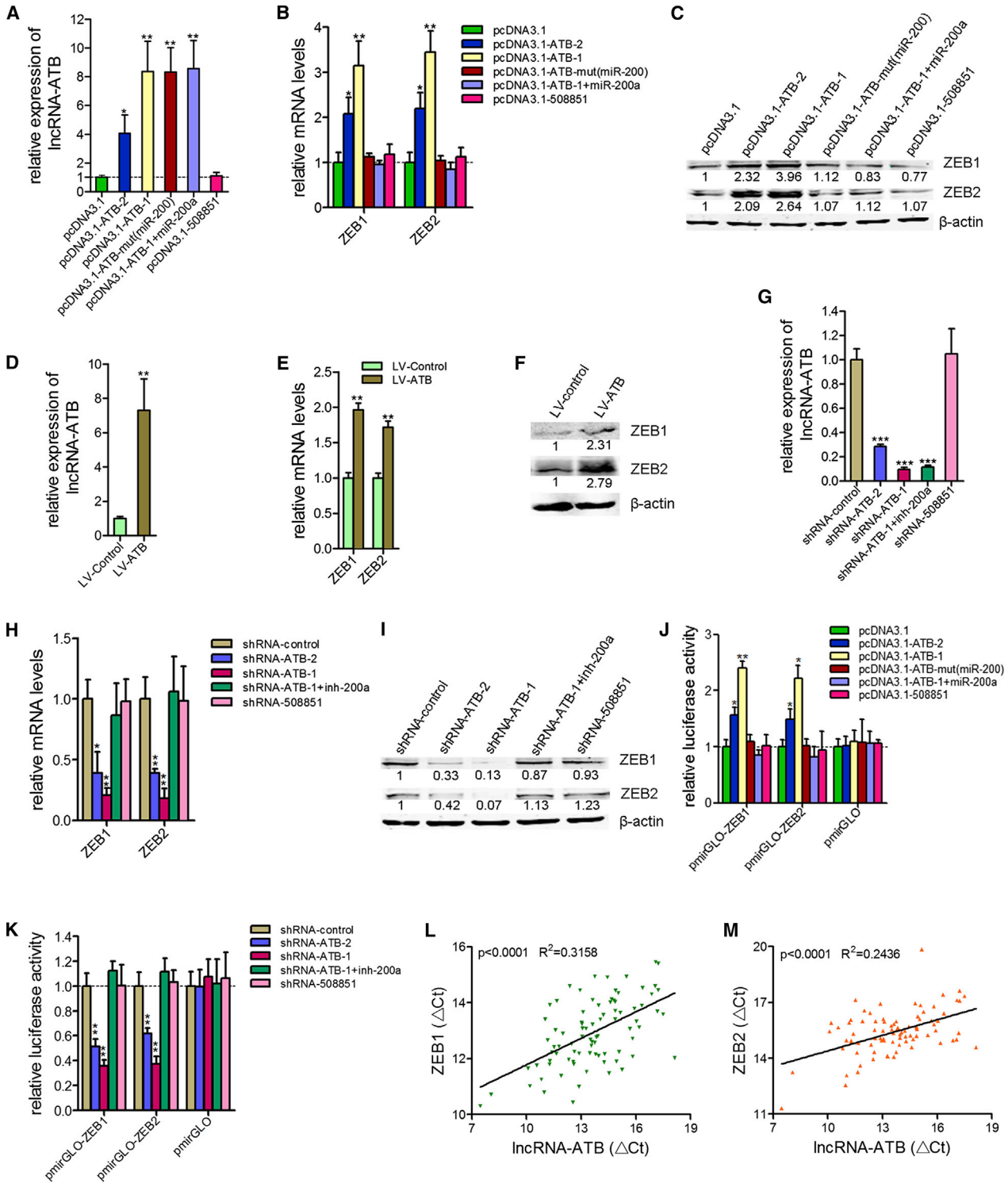

Figure 2. Regulation of ZEB1 and ZEB2 by lncRNA-ATB

(A) The expression of lncRNA-ATB in stable SMMC-7721 cell clones.

(B and C) The mRNA (B) or protein (C) levels of ZEB1 and ZEB2 in stable SMMC-7721 cell clones.

(D) The expression of lncRNA-ATB in stable QSG-7701 cell clones.

(E and F) The mRNA (E) or protein (F) levels of ZEB1 and ZEB2 in stable QSG-7701 cell clones.

(G) The expression of lncRNA-ATB in stable HCCLM6 cell clones.

(H and I) The mRNA (H) or protein (I) levels of ZEB1 and ZEB2 in stable HCCLM6 cell clones.

(legend continued on next page)

miR-200a with a similar overexpression level to the lncRNA-ATB and miR-200a simultaneously overexpressed clone 1 (Figure S3I). Our results indicate that overexpression of lncRNA-ATB rescued the downregulation of ZEB1 and ZEB2 and the inhibition of EMT caused by ectopic expression of miR-200a (Figures S3J and S3K). Taken together, these data suggest a functional role for lncRNA-ATB in inducing EMT. This inducing effect depends on the competitive binding of miR-200s.

Consistent with the different expression of lncRNA-ATB in the four HCC cells in Figure S1M, the expression of ZEB1, ZEB2, N-cadherin, and vimentin were higher and the expression of E-cadherin and ZO-1 were lower in lncRNA-ATB high expression cells (Figure S3L), indicating the expression of lncRNA-ATB was correlated with ZEB1, ZEB2, and EMT features.

To evaluate whether lncRNA-ATB overexpression induced global EMT-related changes, we performed gene expression microarray analysis on lncRNA-ATB overexpressed SMMC-7721 cells. GSEA indicated that three published EMT gene signatures (Alonso et al., 2007; Gotzmann et al., 2006; Huang et al., 2012) were significantly enriched in lncRNA-ATB overexpressed cells (Figure 3J), strongly suggesting that lncRNA-ATB overexpression induces a pervasive and sustained EMT signaling program.

To ascertain the pathological correlation between lncRNA-ATB and EMT in human HCC samples, we measured E-cadherin mRNA level in the same set of 86 HCC tissues shown in Figure 2L and found that lncRNA-ATB transcript level was inversely correlated with E-cadherin mRNA level (Figure 3K), consistent with a role of lncRNA-ATB in EMT.

To directly test whether lncRNA-ATB could promote invasive behavior by promoting EMT-like morphological changes, we determined the invasion ability of different SMMC-7721 and HCCLM6 cell clones using Matrigel-coated transwell experiments. We observed that overexpression of lncRNA-ATB, but not the mutant or lncRNA-508851, significantly increased the invasion potential of SMMC-7721 cells, and this invasion potential was completely abolished when miR-200a was overexpressed (Figure 3L). We also found that depletion of lncRNA-ATB, but not lncRNA-508851, reduced the invasion potential of HCCLM6 cells, which was abrogated by inhibition of miR-200a (Figure 3M). Altogether, these results show that lncRNA-ATB induces EMT and promotes a more invasive phenotype by competitively binding miR-200s.

Aberrant Expression of lncRNA-ATB in Human HCC Tissues

To further define the role of lncRNA-ATB in human HCC, we measured lncRNA-ATB expression level in the same set of HCC tissues shown in Figure 2L and in their pair-matched noncancerous hepatic tissues. The lncRNA-ATB transcript level was higher in the HCC tissues than in the paired adjacent noncancerous hepatic tissues (Figure 4A). We next examined the relationship between lncRNA-ATB expression levels and the clinicopathological characteristics of the 86 HCC samples (Table S3). Correlation regression analysis showed that high expression of lncRNA-ATB was significantly correlated with liver cirrhosis ($p = 0.006$), microvascular invasion ($p = 0.000$), macrovascular invasion ($p = 0.000$), and encapsulation ($p = 0.007$). Portal vein tumor thrombus (PVTT) is the main route for intrahepatic metastasis of HCC cells in human patients. We examined the expression of lncRNA-ATB in 40 pairs of PVTT and pair-matched primary tumor tissues. As shown in Figure 4B, the expression level of lncRNA-ATB was significantly higher in the PVTT tissues than in the primary tumor tissues. These data support that a high level of lncRNA-ATB is strongly associated with the metastasis of HCC cells.

We further examined whether the lncRNA-ATB expression level was correlated with the outcome of HCC after hepatectomy. Kaplan-Meier analysis in the 86 patients with HCC revealed that high lncRNA-ATB expression level in HCC tissues significantly correlated with a reduction in recurrence-free survival ($p < 0.001$; Figure 4C) and overall survival ($p = 0.004$; Figure 4D), consistent with the important roles of lncRNA-ATB in the pathogenesis of HCC and the prognosis of HCC.

lncRNA-ATB Promotes the Invasion-Metastasis Cascade of HCC Cells In Vivo

To evaluate the biological functions of lncRNA-ATB in vivo, we inoculated different clones of SMMC-7721 and HCCLM6 cells subcutaneously into nude mice. Neither the overexpression nor the depletion of lncRNA-ATB had a measurable effect on the growth of tumors and the proportion of proliferating (Ki67+) cancer cells (Figures S4A and S4B; data not shown). We then used subcutaneous tumor tissues to establish orthotopic tumor models. In this model system, lncRNA-ATB overexpression effectively promoted intrahepatic, mesenteric, pulmonic, and diaphragmatic metastases in SMMC-7721 cells. However, mutating the miR-200s binding sites or overexpressing miR-200a only partially abolished the prometastatic role of lncRNA-ATB (Figure 5A; Figures S4C and S4D). We next included a stable SMMC-7721 cell clone with inhibition of miR-200a (Figure S4E) and found that inhibition of miR-200a promoted metastases of SMMC-7721 cells, but the prometastatic role is weaker than that of lncRNA-ATB (Figure 5A; Figure S4C). The depletion of lncRNA-ATB inhibited intrahepatic, mesenteric, and pulmonic metastases in HCCLM6 cells, which was also partially abolished by inhibition of miR-200a (Figure 5B). This implies that miR-200s is most likely not the only functional downstream effector of the prometastatic role of lncRNA-ATB.

Because metastasis is a complex multistep process that involves the early step of tumor invasion and the late step of metastatic colonization in distant organs, we aimed to explore the influence of lncRNA-ATB and miR-200s on the different stages of metastasis. We labeled the different clones with green fluorescent protein (GFP) and established orthotopic tumor models,

(J and K) Luciferase activity in stable SMMC-7721 cell clones (J) or HCCLM6 cell clones (K) transfected with luciferase reporters containing ZEB1 3′UTR, ZEB2 3′UTR or nothing. Data are presented as the relative ratio of firefly luciferase activity to renilla luciferase activity. For (A–K), n = 3, mean ± SD. *$p < 0.05$, **$p < 0.01$, ***$p < 0.001$ (Student's t test).

(L and M) The correlation between lncRNA-ATB transcript level and ZEB1 (L) or ZEB2 (M) mRNA level was measured in 86 HCC tissues. The ΔCt values (normalized to 18S rRNA) were subjected to Pearson correlation analysis.

See also Figure S2.

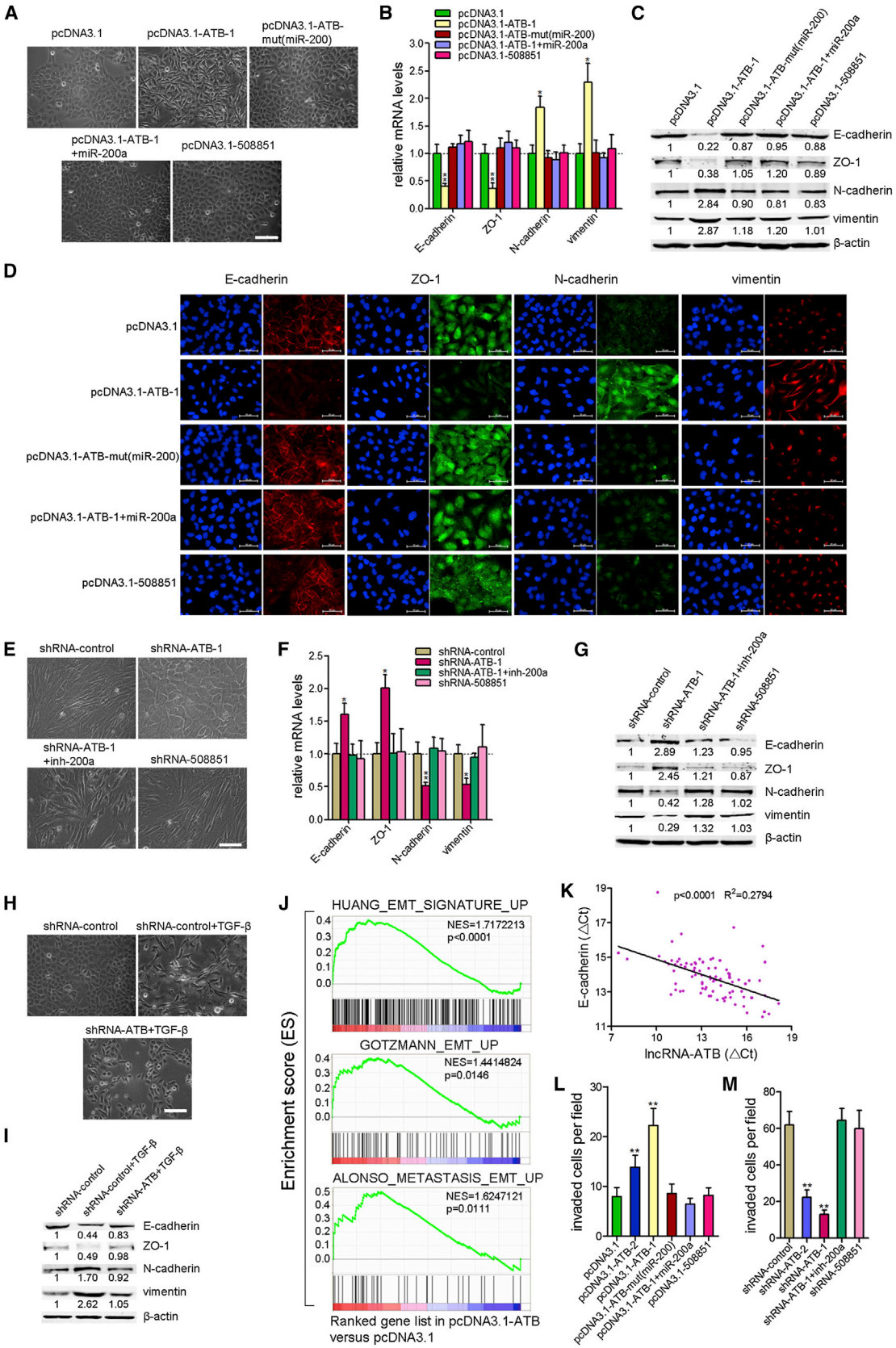

(legend on next page)

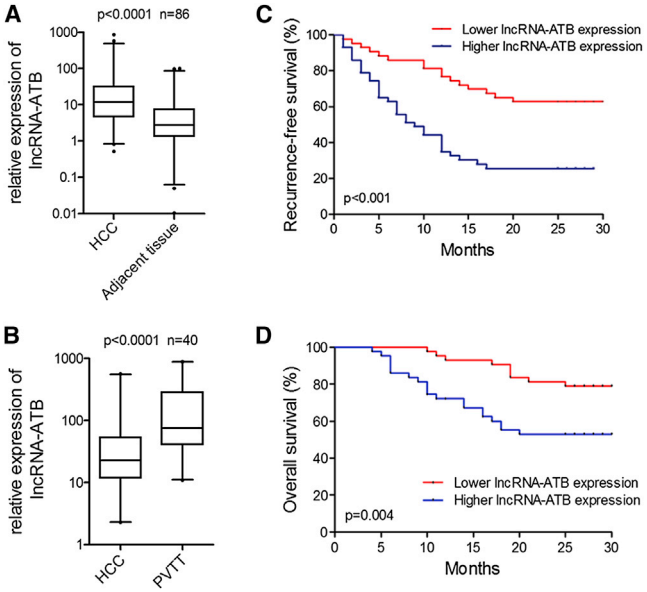

Figure 4. Aberrant Expression of lncRNA-ATB in Clinical Samples

(A) lncRNA-ATB expression in human HCC tissues and paired adjacent noncancerous hepatic tissues. (B) lncRNA-ATB expression in PVTT tissues and paired primary HCC tissues. For (A) and (B), the expression level of lncRNA-ATB was analyzed by qRT-PCR. The horizontal lines in the box plots represent the medians, the boxes represent the interquartile range, and the whiskers represent the 2.5th and 97.5th percentiles. The significant differences between samples were analyzed using the Wilcoxon signed-rank test.

(C and D) Kaplan-Meier analyses of the correlations between lncRNA-ATB expression level and recurrence-free survival (C) or overall survival (D) of 86 patients with HCC. The median expression level was used as the cutoff. Patients with lncRNA-ATB expression values below the 50th percentile were classified as having lower lncRNA-ATB levels. Patients with lncRNA-ATB expression values above the 50th percentile were classified as having higher lncRNA-ATB levels.

See also Table S3.

and 5 weeks later examined circulating tumor cells (CTCs) by flow cytometry from whole-blood samples. As shown in Figure 5C and Figure S4F, ectopic expression of lncRNA-ATB significantly increased the number of CTCs, and the mutation of the miR-200s binding sites or overexpressing miR-200a completely abolished the increase. Inhibition of miR-200a also increased the number of CTCs, which is comparable to that of overexpression of lncRNA-ATB. Reciprocally, the depletion of lncRNA-ATB significantly decreased the number of CTCs, which was abolished by inhibition of miR-200a (Figure 5D). We also analyzed the levels of human LINE1 DNA, another indicator of CTCs, by qPCR of genomic DNA from whole-blood samples. The results were consistent with that of measuring GFP-positive CTCs (Figures 5E and 5F). These data demonstrated that lncRNA-ATB promoted intravasation of HCC cells, which was dependent on the competitive binding of miR-200s.

Consistent with in vitro results, ZEB1, ZEB2, N-cadherin, and vimentin were upregulated, and E-cadherin and ZO-1 were reduced in the orthotopic tumor tissues with lncRNA-ATB overexpression or miR-200a inhibition. In addition, the mutation of the miR-200s binding sites or overexpression of miR-200a completely abolished the effects (Figures S4G–S4J). These data suggest that lncRNA-ATB upregulates ZEB1 and ZEB2, induces EMT, and promotes tumor invasion in vivo, all of which depend on miR-200s.

To explore the influence of lncRNA-ATB on liver colonization, we labeled the different clones with firefly luciferase and inoculated cells intrasplenically into nude mice. Overexpression of lncRNA-ATB resulted in greater liver metastases burden. The mutation of the miR-200s binding sites or overexpression of miR-200a, which induced MET in the liver metastases (Figure S4K), however, did not change this liver metastases-promoting role of lncRNA-ATB. Inhibition of miR-200a also did not influence liver metastases (Figures 5G and 5H; Figures S4L and S4M). The depletion of lncRNA-ATB reduced the liver metastases burden of HCCLM6 cells, which was also not abolished by inhibition of miR-200a (Figures 5I and 5J; Figures S4N and S4O). We further explored the role of lncRNA-ATB in lung colonization by inoculating cells directly into the tail veins of nude mice. We also observed an increase in the lung metastases burden generated by lncRNA-ATB-overexpressing SMMC-7721 cells. The mutation of the miR-200s binding sites or overexpression of miR-200a did not abolish this lung metastases-promoting role of lncRNA-ATB. Inhibition of miR-200a also did not influence lung metastases (Figures 5K and 5L; Figures S4P and S4Q). Reciprocally, the depletion of lncRNA-ATB significantly reduced the lung metastases burden of HCCLM6 cells, which was also not abolished by inhibition of miR-200a (Figures 5M and 5N; Figures S4R and S4S). These results demonstrate that lncRNA-ATB promotes the liver and lung colonization of HCC cells and that this effect is not dependent on miR-200s or EMT. This suggests that other genes or signaling pathways are likely to mediate the procolonization efficiency of lncRNA-ATB. Consistent with in vitro invasion assay results, the in vivo results also indicated that HCCLM6 is highly metastatic compared with SMMC-7721 cells.

Figure 3. The Effects of lncRNA-ATB on EMT and Invasion In Vitro

(A) Phase-contrast micrographs of indicated SMMC-7721 cell clones. Scale bars = 100 μm.

(B and C) The mRNA (B) or protein (C) levels of EMT markers in indicated SMMC-7721 cell clones.

(D) Immunofluorescence microscopy analysis of the localization and expression of EMT markers in indicated SMMC-7721 cell clones. Scale bars = 50 μm.

(E) Phase-contrast micrographs of indicated HCCLM6 cell clones. Scale bars represent 100 μm.

(F and G) The mRNA (F) or protein (G) levels of EMT markers in indicated HCCLM6 cell clones.

(H and I) Phase-contrast micrographs (H) or the protein levels of EMT markers (I) in control and lncRNA-ATB-knockdown SMMC-7721 cells undergoing TGF-induced EMT. Scale bars represent 100 μm.

(J) GSEA of EMT gene signatures in lncRNA-ATB overexpressed SMMC-7721 cells versus control cells. NES, normalized enrichment score.

(K) The correlation between lncRNA-ATB transcript level and E-cadherin mRNA level was measured in 86 HCC tissues. The ΔCt values (normalized to 18S rRNA) were subjected to Pearson correlation analysis.

(L and M) Indicated SMMC-7721 cell clones (L) or HCCLM6 cell clones (M) were added to the top of transwells coated with Matrigel. The number of invasive cells per field was counted after 48 hr. Data are shown as mean ± SD n = 3. *p < 0.05, **p < 0.01 (Student's t test). See also Figure S3.

A

SMMC-7721	Mets	Liver	Mesentery	Lung	Diaphragm
pcDNA3.1	1/10	1/10	0/10	0/10	0/10
pcDNA3.1-ATB-1	9/10**	9/10	5/10	3/10	1/10
pcDNA3.1-ATB-mut(miR-200)	5/10	5/10	2/10	1/10	0/10
pcDNA3.1-ATB-1+miR-200a	5/10	5/10	2/10	1/10	1/10
pcDNA3.1-508851	2/10	2/10	0/10	0/10	0/10
inh-NC	1/10	1/10	0/10	0/10	0/10
inh-200a	5/10	5/10	3/10	2/10	0/10

B

HCCLM6	Mets	Liver	Mesentery	Lung
shRNA-control	8/10	8/10	5/10	3/10
shRNA-ATB-1	1/10**	1/10	0/10	0/10
shRNA-ATB-1+inh-200a	4/10	4/10	2/10	1/10
shRNA-508851	9/10	9/10	5/10	4/10

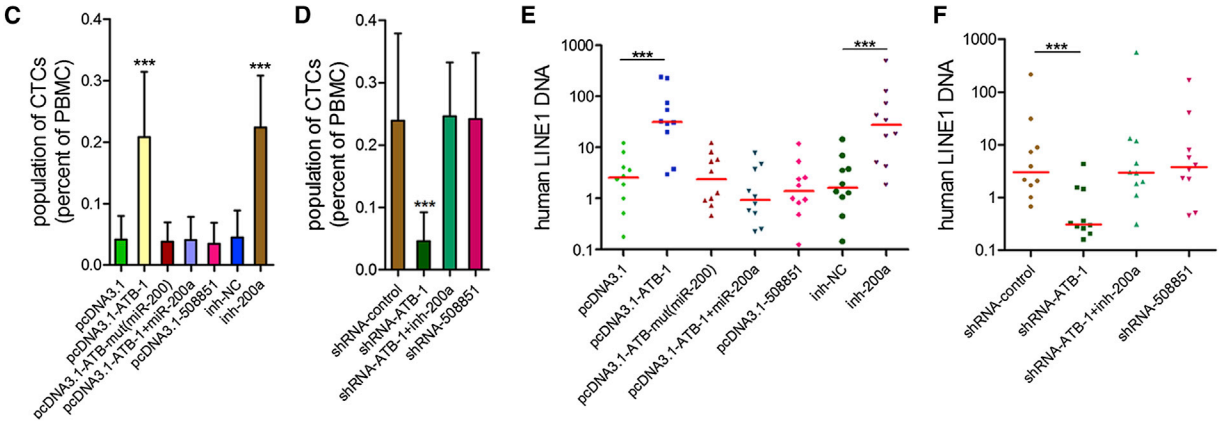

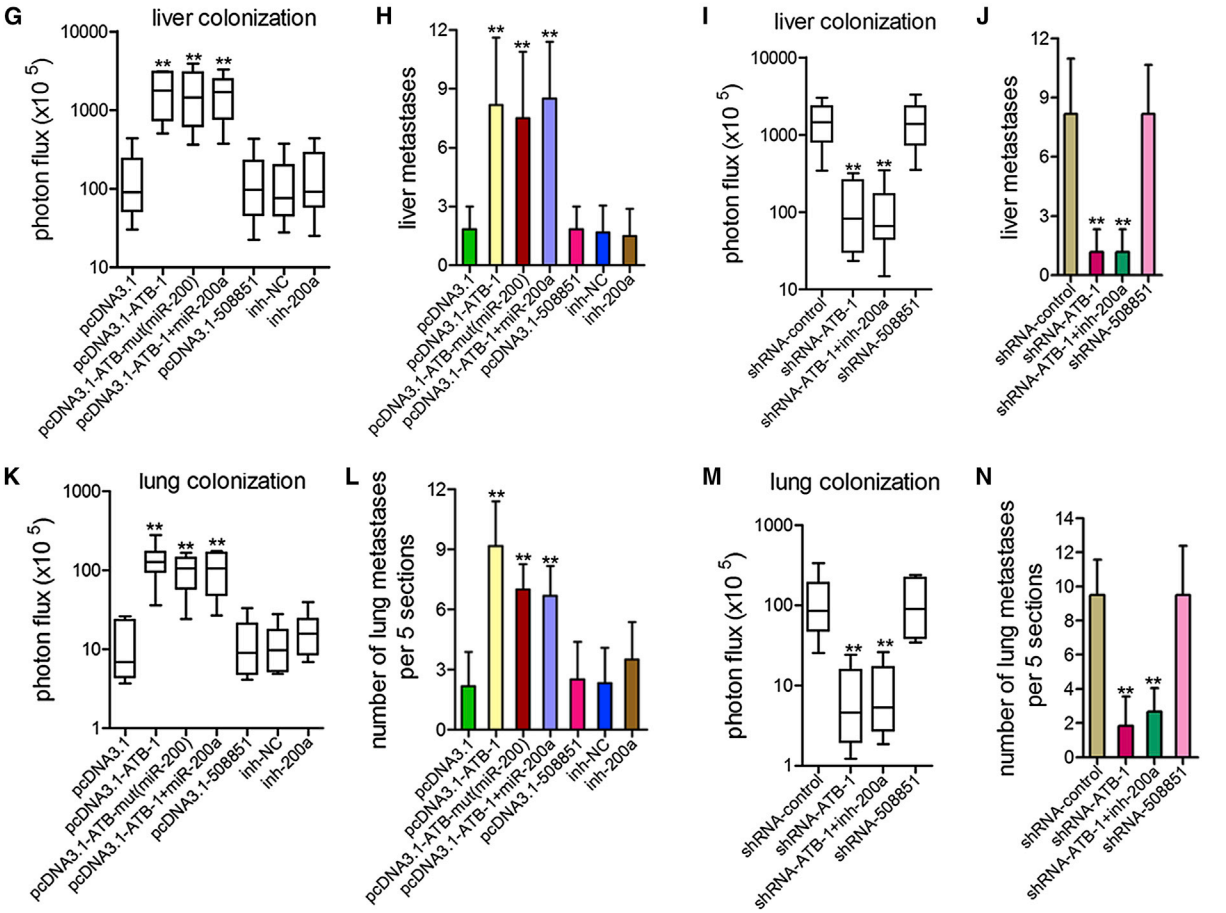

(legend on next page)

lncRNA-ATB Interacts with and Increases Stability of IL-11 mRNA

We next sought to explore the mechanisms behind the potent effect of lncRNA-ATB on metastatic colonization. Recently, many lncRNAs have been reported to interact with mRNA and increase the stability of mRNA (Faghihi et al., 2008; Yoon et al., 2012). To identify mRNA species bound by lncRNA-ATB, we performed an RIP to pull down endogenous mRNAs associated with lncRNA-ATB (Figure 6A) and sequenced the retrieved RNA. Interleukin-11 (IL-11) was one of the most enriched transcripts (Figure 6B; Figure S5A; Table S4), which has been reported to activate STAT3 signaling and confer a survival advantage to metastatic cells (Calon et al., 2012). Furthermore, GSEA indicated that KEGG_JAK_STAT signaling pathway from the Molecular Signatures Database (Liberzon et al., 2011) and published distinct IL-11/STAT3 upregulated gene signatures (Azare et al., 2007; Dauer et al., 2005; Putoczki et al., 2013) were significantly enriched in lncRNA-ATB overexpressed cells, whereas IL-11/STAT3 downregulated gene signature was negatively enriched (Figure 6C). We thus reasoned that lncRNA-ATB may promote metastatic cell survival through IL-11 mRNA binding, autocrine induction of IL-11, and activation of IL-11/STAT3 signaling. Promisingly, we discovered that the liver metastases generated in the intrasplenically inoculated model displayed higher expression of IL-11 and more accumulation of p-STAT3 when derived from the lncRNA-ATB-overexpressing SMMC-7721 cells, and lower expression of IL-11 and less accumulation of p-STAT3 derived from lncRNA-ATB-downregulated HCCLM6 cells (Figures S5B and S5C).

Using BLAST (http://blast.ncbi.nlm.nih.gov/), we identified six regions of high complementary between lncRNA-ATB and IL-11 mRNA, but none for β-actin mRNA (Figure 6D). We then mutated all six binding sites in lncRNA-ATB. To validate the direct interaction of lncRNA-ATB with IL-11 mRNA, we performed RIP-qPCR and the results demonstrated that the lncRNA-ATB RIP in SMMC-7721 cells is significantly enriched for IL-11 mRNA compared to the empty vector, IgG, β-actin mRNA, IL-11 binding sites mutated lncRNA-ATB (lncRNA-ATB-mut(IL-11)), or lncRNA-508851, which did not have a complementary region with IL-11 mRNA (Figure 6E). The specific association between lncRNA-ATB and IL-11 mRNA was further validated by affinity pull-down of endogenous IL-11 mRNA using in vitro transcribed biotin-labeled lncRNA-ATB (Figure 6F). These results suggest that lncRNA-ATB interacts with IL-11 mRNA.

To test whether lncRNA-ATB regulates the stability of IL-11 mRNA, we treated different clones of SMMC-7721 and HCCLM6 cells with α-amanitin to block new RNA synthesis and then measured the loss of IL-11, β-actin, and 18S rRNA over a 24 hr period. The overexpression of lncRNA-ATB, but not lncRNA-ATB-mut(IL-11) or lncRNA-508851, elongated the half-life of IL-11 mRNA, and conversely, the depletion of lncRNA-ATB shortened the half-life of IL-11 mRNA (Figure 6G). Collectively, these data demonstrate that lncRNA-ATB specially increases the stability of IL-11 mRNA, which depends on the binding of IL-11 mRNA.

lncRNA-ATB Activates IL-11/STAT3 Signaling

To further validate the effects of lncRNA-ATB on IL-11/STAT3 signaling in vitro, we measured IL-11 mRNA levels in different clones of SMMC-7721 and HCCLM6 cells and found that the overexpression of lncRNA-ATB, but not lncRNA-ATB-mut(IL-11) or lncRNA-508851, significantly increased IL-11 mRNA levels in a dose-dependent manner, and ectopic expression of miR-200a did not change the effects (Figure 6H). Reciprocally, the depletion of lncRNA-ATB significantly reduced IL-11 mRNA levels in a dose-dependent manner, which was also not changed by inhibition of miR-200a (Figure 6I). Consistent with the different expression of lncRNA-ATB in the four HCC cells in Figure S1M, the expression of IL-11 was higher in lncRNA-ATB high expression cells (Figure S5D). We also found that overexpression of lncRNA-ATB upregulated IL-11 mRNA level in QSG-7701 cells (Figure S5E). To examine whether lncRNA-ATB increases IL-11 secretion and activates IL-11/STAT3 signaling, we measured IL-11 levels in the cell supernatants and phosphorylation levels of STAT3 in different clones. The overexpression of lncRNA-ATB, but not lncRNA-ATB-mut(IL-11) or lncRNA-508851, leads to increased IL-11 levels in the cell supernatants and phosphorylation levels of STAT3 in a dose-dependent manner (Figures 6J and 6K). Reciprocally, the depletion of lncRNA-ATB leads to reduced IL-11 levels in the cell supernatants and phosphorylation levels of STAT3 in a dose-dependent manner (Figures 6L and 6M). Neither overexpression nor inhibition of miR-200a changed the effects (Figures 6J–6M). Overexpression of lncRNA-ATB also upregulated IL-11 levels in the cell

Figure 5. The Roles of lncRNA-ATB in the Invasion-Metastasis Cascade of HCC Cells

(A and B) Incidence of metastases 8 weeks after orthotopic xenografting in nude mice using indicated SMMC-7721 cell clones (A) or HCCLM6 cell clones (B) (Fisher's exact test).

(C and D) The number of GFP labeled CTCs was examined by flow cytometry from whole-blood samples 5 weeks after orthotopic xenografting using indicated SMMC-7721 cell clones (C) or HCCLM6 cell clones (D). PBMC, peripheral blood mononuclear cells.

(E and F) Relative levels of human LINE1 DNA were analyzed by qPCR of genomic DNA from the blood in (C) and (D), normalized to mouse LINE1 DNA. For (C–F), n = 10, nonparametric Mann-Whitney U test.

(G) Luciferase signal intensities of mice in each group 6 weeks after intrasplenic injection with 2×10^6 indicated SMMC-7721 cells. The horizontal lines in the box plots represent the medians, the boxes represent the interquartile range, and the whiskers represent the minimum and maximum values.

(H) Number of liver metastases in mice from (G).

(I) Luciferase signal intensities of mice in each group 6 weeks after intrasplenic injection with 2×10^6 indicated HCCLM6 cells. Data are shown as in (G).

(J) Number of liver metastases in mice from (I).

(K) Luciferase signal intensities of mice in each group 5 weeks after tail vein injection with 1×10^6 indicated SMMC-7721 cells. Data are shown as in (G).

(L) Number of metastatic nodules in the lungs from the mice in (K) (five sections evaluated per lung).

(M) Luciferase signal intensities of mice in each group 5 weeks after tail vein injection with 1×10^6 indicated HCCLM6 cells. Data are shown as in (G).

(N) Number of metastatic nodules in the lungs from the mice in (M) (five sections evaluated per lung). For (G–N), n = 6, nonparametric Mann-Whitney U test. Bars represent mean ± SD. $^{**}p < 0.01$, $^{***}p < 0.001$. See also Figure S4.

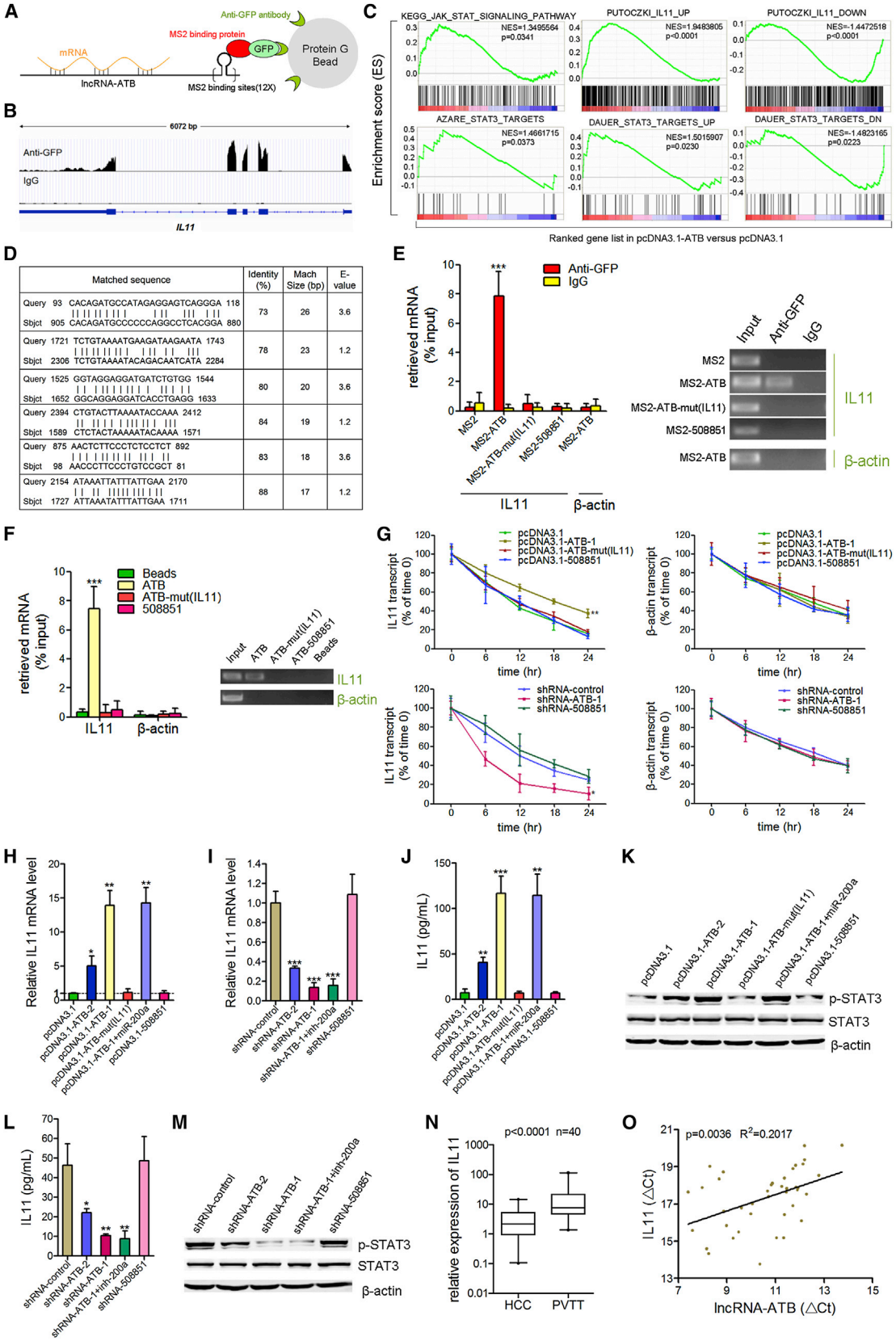

(legend on next page)

supernatants and phosphorylation levels of STAT3 in QSG-7701 cells (Figures S5F and S5G). STAT3 downstream target protein BCL2 was also upregulated by overexpression of lncRNA-ATB, but not lncRNA-ATB-mut(IL-11) or lncRNA-508851, and was downregulated by depletion of lncRNA-ATB (Figures S5H–S5J). These results indicate that lncRNA-ATB upregulated the expression of IL-11, increased IL-11 secretion, and activated STAT3 signaling in an autocrine manner. The effects of lncRNA-ATB on IL-11/STAT3 signaling are not dependent on miR-200s.

To confirm the regulation of IL-11 by lncRNA-ATB in human HCC tissues, we measured IL-11 mRNA level in the same set of 40 pairs of PVTT and pair-matched primary HCC tissues shown in Figure 4B and found that IL-11 mRNA level was significantly higher in the PVTT tissues than in the primary HCC tissues (Figure 6N). Importantly, the IL-11 mRNA level is correlated with the lncRNA-ATB transcript level in the PVTT tissues (Figure 6O). These clinical data demonstrated that IL-11 may be associated with the metastasis of HCC cells and were consistent with the role of lncRNA-ATB in the regulation of IL-11.

lncRNA-ATB Requires IL-11/STAT3 Signaling to Promote Colonization

To test the contribution of IL-11 to the procolonization role of lncRNA-ATB, we knocked down IL-11 in lncRNA-ATB-overexpressing SMMC-7721 clone 1. This knockdown has no significant effect on lncRNA-ATB expression (Figure 7A). We first measured the effects of IL-11 on EMT, and found that knockdown of IL-11 did not induce or invert EMT (Figure S6A). Next, we found that the mutation of IL-11 binding sites or knockdown of IL-11 also did not change the proinvasive efficiency of lncRNA-ATB (Figure S6B).

The cells were labeled with firefly luciferase and inoculated intrasplenically into nude mice. During the first few days following inoculation, most of the cells that reached the liver were progressively lost, and by 7 days, tumor cells were barely detectable. The overexpression of lncRNA-ATB, but not lncRNA-ATB-mut(IL-11), significantly increased the number of cells detected at the early time points and induced more metastatic foci in the liver at the late time point. The knockdown of IL-11 in lncRNA-ATB-overexpressing cells reduced the amounts to near those of the control cells (Figures 7B–7E). We further explored the role of lncRNA-ATB and IL-11 in lung colonization by injecting cells directly into the tail veins of nude mice. lncRNA-ATB overexpressing cells, but not that of lncRNA-ATB-mut(IL-11), displayed increased lung colonization rates at the early time points and formed more metastatic tumors in the lung at the late time point, whereas knockdown of IL-11 mostly abolished this increase (Figures 7F–7I). These data demonstrated that lncRNA-ATB enhances the colonization potential of HCC cells and this effect depends on IL-11.

DISCUSSION

In this study, we report that lncRNA-ATB, which could be activated by TGF-β, promotes HCC cell invasion by competitively binding the miR-200 family, upregulating ZEB1 and ZEB2, and then inducing EMT. On the other hand, lncRNA-ATB promotes HCC cell colonization at the site of metastasis by binding IL-11 mRNA, increasing IL-11 mRNA stability, causing autocrine induction of IL-11, and then activating STAT3 signaling. Therefore, lncRNA-ATB plays a prometastatic role in HCC (Figure 8). We also found that the expression of lncRNA-ATB was increased in HCC and was further increased in PVTT. Furthermore, a higher level of lncRNA-ATB was associated with tumor invasion in patients with HCC and was inversely correlated with prognosis. All these data support our conclusion that lncRNA-ATB has pleiotropic effects on HCC cell invasion, colonization, and metastasis. Therefore, lncRNA-ATB was determined to have oncogenic activity.

Our results indicated that a higher level of lncRNA-ATB was associated with liver cirrhosis in patients with HCC, which is consistent with the observation that TGF-β is also associated with liver cirrhosis (Yang et al., 2013). A recent report indicated that the level of TGF-β signaling activity was higher in PVTT tissues than the primary HCC tissues (Yang et al., 2012), which further supports the regulation of lncRNA-ATB by TGF-β in vivo. The biphasic activities of the TGF-β signaling pathway during

Figure 6. lncRNA-ATB Interacts with IL-11 mRNA and Activates IL-11/STAT3 Signaling in HCC Cells

(A) A schematic outline of the MS2-RIP strategy used to identify endogenous mRNA:lncRNA-ATB binding.

(B) lncRNA-ATB-MS2 RIP-seq identification of IL-11 enrichment in anti-GFP and nonspecific IgG groups.

(C) GSEA of KEGG_JAK_STAT signaling pathway and published IL-11/STAT3 regulated gene signatures in lncRNA-ATB overexpressed SMMC-7721 cells versus control cells. NES, normalized enrichment score.

(D) Regions of putative interaction between lncRNA-ATB (query) and IL-11 mRNA (subject).

(E) RIP-derived RNA was measured by qRT-PCR. The levels of qRT-PCR products were expressed as a percentage of input RNA.

(F) SMMC-7721 cell lysates were incubated with biotin-labeled lncRNA-ATB; after pull-down, mRNA was extracted and assessed by qRT-PCR. Data are shown as in (E).

(G) The stability of IL-11 and β-actin mRNA over time was measured by qRT-PCR relative to time 0 after blocking new RNA synthesis with α-amanitin (50 μM) in indicated SMMC-7721 cell clones or HCCLM6 cell clones and normalized to 18S rRNA (a product of RNA polymerase I that is unchanged by α-amanitin).

(H and I) Relative IL-11 mRNA levels in indicated SMMC-7721 cell clones (H) or HCCLM6 cell clones (I).

(J and K) Concentration of IL-11 in the culture medium measured by ELISA (J) or p-STAT3 levels determined by western blot (K) from indicated SMMC-7721 cell clones.

(L and M) Concentration of IL-11 in the culture medium measured by ELISA (L) or p-STAT3 levels determined by western blot (M) from indicated HCCLM6 cell clones. For (E–M), n = 3, mean ± SD, Student's t test, *$p < 0.05$, **$p < 0.01$, ***$p < 0.001$.

(N) IL-11 mRNA levels in primary HCC and PVTT tissues from the same set of patients as in Figure 4B were measured by qRT-PCR. The horizontal lines in the box plots represent the medians, the boxes represent the interquartile range, and the whiskers represent the 2.5th and 97.5th percentiles. Wilcoxon signed-rank test.

(O) The correlation between lncRNA-ATB transcript level and IL-11 mRNA level was measured in the same set of PVTT tissues as in (N). The ΔCt values (normalized to 18S rRNA) were subjected to Pearson correlation analysis.

See also Figure S5 and Table S4.

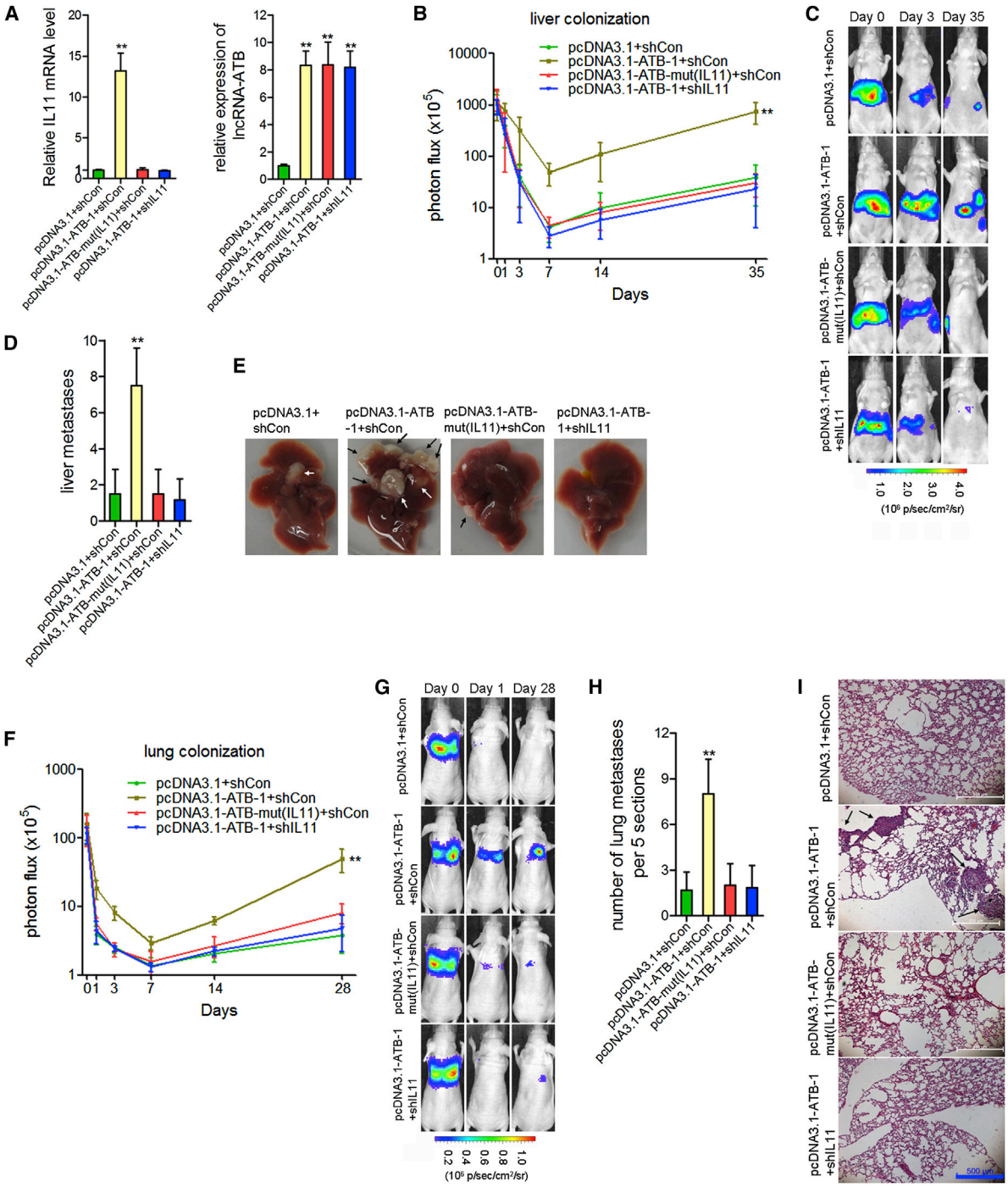

Figure 7. The Pro-Colonization Role of lncRNA-ATB Requires IL-11/STAT3 Signaling

(A) The expression levels of IL-11 and lncRNA-ATB were determined by qRT-PCR. n = 3, Student's t test.

(B) Luciferase signal intensities of the mice in each group over time after intrasplenic injection with 2 × 10^6 indicated SMMC-7721 cell clones.

(C) Representative images of mice from (B) over time.

(D) The number of liver metastases in the mice from (B) 35 days after intrasplenic injection.

(E) Representative livers from (D).

(F) Luciferase signal intensities of mice over time after tail vein injection with 1 × 10^6 indicated SMMC-7721 cell clones.

(G) Representative images of the mice from (F) over time.

(H) The number of metastatic nodules in the lungs from (F) 28 days after tail vein injection (five sections evaluated per lung).

(I) Hematoxylin and eosin-stained images of lung tissues isolated from the mice in (H). Scale bars represent 500 μm. For (B–I), n = 6, nonparametric Mann-Whitney U test; arrows indicate the metastasis nodules. Data are shown as mean ± SD, **p < 0.01. See also Figure S6.

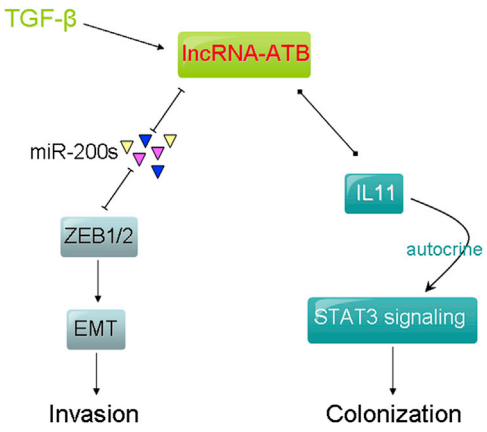

Figure 8. A Schematic Model of lncRNA-ATB Functions during the Invasion-Metastasis Cascade

lncRNA-ATB, which could be activated by TGF-β, promotes HCC cell invasion by competitively binding the miR-200 family, upregulating ZEB1 and ZEB2, and then inducing EMT. On the other hand, lncRNA-ATB promotes HCC cell colonization at the site of metastases by binding IL-11 mRNA, increasing IL-11 mRNA stability, causing autocrine induction of IL-11, and then activating STAT3 signaling.

tumorigenesis hinder its utilization in clinical treatment. Therefore, it would be beneficial to target the tumor-progressing arm of TGF-β action while avoiding the tumor-suppressing arm. Thus, the specific downstream effectors of the different TGF-β signaling pathways need to be explored further. In this study, we identified that lncRNA-ATB mediates the role of TGF-β in inducing EMT and promoting metastasis. Promisingly, lncRNA-ATB was activated by TGF-β and induced EMT not only in HCC cells, but also in colorectal cancer and breast cancer cells, indicating that lncRNA-ATB is a more general TGF-β mediator. Our results indicated that a short-term TGF-β treatment was sufficient to activate lncRNA-ATB, which implied that lncRNA-ATB may be a direct target of TGF-β/Smad pathway, but how TGF-β activates lncRNA-ATB requires further investigation.

In this study, we found that lncRNA-ATB shares miR-200s response elements with ZEB1 and ZEB2, the master inducers of EMT. In our in vitro system, an orthotopic xenograft model of nude mice and clinical HCC tissues, we observed that ectopic expression of lncRNA-ATB was sufficient to increase ZEB1 and ZEB2 and induce EMT. The mRNA expression profile after overexpressing of lncRNA-ATB fortified its role in inducing EMT. Notably, this role depends on the competitive binding of miR-200s, indicating that lncRNA-ATB functions as a ceRNA. Because there is a double negative feedback loop between miR-200s and ZEB1/ZEB2 (Burk et al., 2008), the upregulation of ZEB1 and ZEB2 by lncRNA-ATB could further augment the effects. It is widely recognized that EMT facilitates tumor invasion and dissemination (Massagué, 2008). Consistently, in our in vitro system, an orthotopic xenograft model of nude mice and clinical HCC tissues, we all found that by inducing EMT, lncRNA-ATB promotes HCC cell invasion.

In the orthotopic xenograft model in nude mice, we found that lncRNA-ATB promoted HCC cell metastases, which were not completely dependent on miR-200s or EMT. This implies that metastasis is not only determined by the invasion potential and that the miR-200-ZEB-EMT axis is not the only downstream effector of lncRNA-ATB. Metastasis is a complex multistep process that involves early invasion and late colonization of cancer cells (Tao et al., 2013). Clinical observations and animal model studies have indicated that, despite the significant and continuous tumor cell intravasation into the circulation, only a small minority of these cells colonize a distant organ (Gupta and Massagué, 2006). Therefore, colonization is a rather inefficient process and also has a critical influence on ultimate metastasis. In our tail vein injection and intrasplenic inoculation xenograft models, we found that the miR-200-EMT axis had no significant effect on colonization. Therefore, lncRNA-ATB exerts its procolonization effect through other pathways.

We combined RIP-seq and transcriptome analysis to identify that lncRNA-ATB bound IL-11 mRNA, increased IL-11 mRNA stability, and caused autocrine induction of IL-11, and activated IL-11/STAT3 signaling, which were further verified in our in vitro system, the xenograft metastasis model, and clinical HCC tissues. In our xenograft model using nude mice, IL-11 secreted by HCC cells contributes to the procolonization role of lncRNA-ATB, because the depletion of IL-11 in HCC cells abolished the procolonization effect of lncRNA-ATB. The depletion of IL-11 did not induce or invert EMT, indicating that the role of lncRNA-ATB or IL-11 in colonization is not dependent on EMT or MET.

Taken together, our research demonstrated that lncRNA-ATB acts as a key regulator of TGF-β signaling pathways and revealed roles of TGF-β in regulating long noncoding RNAs. The findings of this study have significant implications regarding our understanding of HCC metastasis pathogenesis. As direct targets of lncRNA-ATB, miR-200-ZEB and IL-11 mediated the role of lncRNA-ATB in local invasion and distant colonization, respectively. The pleiotropic effects of lncRNA-ATB on the early and late steps of the invasion-metastasis cascade suggest that lncRNA-ATB could be an effective target for antimetastasis therapies.

EXPERIMENTAL PROCEDURES

Patients

Frozen HCC tissues, normal liver tissues, and PVTT tissues were randomly obtained with informed consent from patients who underwent radical resections in the Eastern Hepatobiliary Surgery Hospital (Second Military Medical University, Shanghai, China). Ethical consent was granted from the Committees for Ethical Review of Research involving Human Subjects of Second Military Medical University.

Animal Studies

The animal studies were approved by the Institutional Animal Care and Use Committee of the Second Military Medical University. Male athymic BALB/c nude mice (4–5 weeks old) were used for animal studies. Subcutaneous tumor growth assays were performed as previously described (Yuan et al., 2011). Orthotopic xenograft model and metastasis model are described in the Supplemental Experimental Procedures.

Statistical Analysis

All statistical analyses were performed using the GraphPad Prism Software (GraphPad Software). For comparisons, Student's t test (two-tailed), Wilcoxon signed-rank test, Pearson chi-square test, Pearson correlation analysis, Log-rank test, Fisher's exact test, and nonparametric Mann-Whitney U test were performed as indicated. A p value < 0.05 was considered significant.

ACCESSION NUMBERS

The Gene Expression Omnibus accession numbers for the lncRNA microarray data for TGF-β-treated cells, gene expression data for lncRNA-ATB overexpressed SMMC-7721 cells, and RIP-seq data of lncRNA-ATB are GSE54797, GSE54798, and GSE54799, respectively.

SUPPLEMENTAL INFORMATION

Supplemental Information includes Supplemental Experimental Procedures, six figures, and four tables and can be found with this article online at http://dx.doi.org/10.1016/j.ccr.2014.03.010.

ACKNOWLEDGMENTS

We thank Dr. Xing He from Department of Tropical Infectious Diseases, Second Military Medical University for technical assistance and Dr. Xiao-zhi Wang from Gminix (Shanghai, China) for assistance with bioinformatic analyses. This work was supported by grants from the National Natural Science Foundation of China (grant nos. 81330037, 81372240, 81071680, 81071700, 81171936, 81171937, and 31171251), the National Natural Science Foundation of Shanghai (12ZR1437200), and the Youth start-up funding of SMMU (2011QN02).

Received: June 29, 2013
Revised: January 7, 2014
Accepted: March 11, 2014
Published: April 24, 2014

REFERENCES

Akhurst, R.J., and Hata, A. (2012). Targeting the TGFβ signalling pathway in disease. Nat. Rev. Drug Discov. *11*, 790–811.

Alonso, S.R., Tracey, L., Ortiz, P., Pérez-Gómez, B., Palacios, J., Pollán, M., Linares, J., Serrano, S., Sáez-Castillo, A.I., Sánchez, L., et al. (2007). A high-throughput study in melanoma identifies epithelial-mesenchymal transition as a major determinant of metastasis. Cancer Res. *67*, 3450–3460.

Azare, J., Leslie, K., Al-Ahmadie, H., Gerald, W., Weinreb, P.H., Violette, S.M., and Bromberg, J. (2007). Constitutively activated Stat3 induces tumorigenesis and enhances cell motility of prostate epithelial cells through integrin beta 6. Mol. Cell. Biol. *27*, 4444–4453.

Budhu, A., Forgues, M., Ye, Q.H., Jia, H.L., He, P., Zanetti, K.A., Kammula, U.S., Chen, Y., Qin, L.X., Tang, Z.Y., and Wang, X.W. (2006). Prediction of venous metastases, recurrence, and prognosis in hepatocellular carcinoma based on a unique immune response signature of the liver microenvironment. Cancer Cell *10*, 99–111.

Burk, U., Schubert, J., Wellner, U., Schmalhofer, O., Vincan, E., Spaderna, S., and Brabletz, T. (2008). A reciprocal repression between ZEB1 and members of the miR-200 family promotes EMT and invasion in cancer cells. EMBO Rep. *9*, 582–589.

Calon, A., Espinet, E., Palomo-Ponce, S., Tauriello, D.V., Iglesias, M., Céspedes, M.V., Sevillano, M., Nadal, C., Jung, P., Zhang, X.H., et al. (2012). Dependency of colorectal cancer on a TGF-β-driven program in stromal cells for metastasis initiation. Cancer Cell *22*, 571–584.

Cesana, M., Cacchiarelli, D., Legnini, I., Santini, T., Sthandier, O., Chinappi, M., Tramontano, A., and Bozzoni, I. (2011). A long noncoding RNA controls muscle differentiation by functioning as a competing endogenous RNA. Cell *147*, 358–369.

Dauer, D.J., Ferraro, B., Song, L., Yu, B., Mora, L., Buettner, R., Enkemann, S., Jove, R., and Haura, E.B. (2005). Stat3 regulates genes common to both wound healing and cancer. Oncogene *24*, 3397–3408.

Faghihi, M.A., Modarresi, F., Khalil, A.M., Wood, D.E., Sahagan, B.G., Morgan, T.E., Finch, C.E., St Laurent, G., 3rd, Kenny, P.J., and Wahlestedt, C. (2008). Expression of a noncoding RNA is elevated in Alzheimer's disease and drives rapid feed-forward regulation of beta-secretase. Nat. Med. *14*, 723–730.

Fidler, I.J. (2003). The pathogenesis of cancer metastasis: the 'seed and soil' hypothesis revisited. Nat. Rev. Cancer *3*, 453–458.

Gotzmann, J., Fischer, A.N., Zojer, M., Mikula, M., Proell, V., Huber, H., Jechlinger, M., Waerner, T., Weith, A., Beug, H., and Mikulits, W. (2006). A crucial function of PDGF in TGF-beta-mediated cancer progression of hepatocytes. Oncogene *25*, 3170–3185.

Gregory, P.A., Bert, A.G., Paterson, E.L., Barry, S.C., Tsykin, A., Farshid, G., Vadas, M.A., Khew-Goodall, Y., and Goodall, G.J. (2008). The miR-200 family and miR-205 regulate epithelial to mesenchymal transition by targeting ZEB1 and SIP1. Nat. Cell Biol. *10*, 593–601.

Gupta, G.P., and Massagué, J. (2006). Cancer metastasis: building a framework. Cell *127*, 679–695.

Gupta, R.A., Shah, N., Wang, K.C., Kim, J., Horlings, H.M., Wong, D.J., Tsai, M.C., Hung, T., Argani, P., Rinn, J.L., et al. (2010). Long non-coding RNA HOTAIR reprograms chromatin state to promote cancer metastasis. Nature *464*, 1071–1076.

Huang, S., Hölzel, M., Knijnenburg, T., Schlicker, A., Roepman, P., McDermott, U., Garnett, M., Grernrum, W., Sun, C., Prahallad, A., et al. (2012). MED12 controls the response to multiple cancer drugs through regulation of TGF-β receptor signaling. Cell *151*, 937–950.

Jemal, A., Bray, F., Center, M.M., Ferlay, J., Ward, E., and Forman, D. (2011). Global cancer statistics. CA Cancer J. Clin. *61*, 69–90.

Kang, Y., Chen, C.R., and Massagué, J. (2003). A self-enabling TGFbeta response coupled to stress signaling: Smad engages stress response factor ATF3 for Id1 repression in epithelial cells. Mol. Cell *11*, 915–926.

Lewis, B.P., Burge, C.B., and Bartel, D.P. (2005). Conserved seed pairing, often flanked by adenosines, indicates that thousands of human genes are microRNA targets. Cell *120*, 15–20.

Liberzon, A., Subramanian, A., Pinchback, R., Thorvaldsdóttir, H., Tamayo, P., and Mesirov, J.P. (2011). Molecular signatures database (MSigDB) 3.0. Bioinformatics *27*, 1739–1740.

Lin, M.F., Jungreis, I., and Kellis, M. (2011). PhyloCSF: a comparative genomics method to distinguish protein coding and non-coding regions. Bioinformatics *27*, i275–i282.

Majumdar, A., Curley, S.A., Wu, X., Brown, P., Hwang, J.P., Shetty, K., Yao, Z.X., He, A.R., Li, S., Katz, L., et al. (2012). Hepatic stem cells and transforming growth factor β in hepatocellular carcinoma. Nat Rev Gastroenterol Hepatol *9*, 530–538.

Massagué, J. (2008). TGFbeta in Cancer. Cell *134*, 215–230.

Mercer, T.R., Dinger, M.E., and Mattick, J.S. (2009). Long non-coding RNAs: insights into functions. Nat. Rev. Genet. *10*, 155–159.

Ocaña, O.H., Córcoles, R., Fabra, A., Moreno-Bueno, G., Acloque, H., Vega, S., Barrallo-Gimeno, A., Cano, A., and Nieto, M.A. (2012). Metastatic colonization requires the repression of the epithelial-mesenchymal transition inducer Prrx1. Cancer Cell *22*, 709–724.

Padua, D., Zhang, X.H., Wang, Q., Nadal, C., Gerald, W.L., Gomis, R.R., and Massagué, J. (2008). TGFbeta primes breast tumors for lung metastasis seeding through angiopoietin-like 4. Cell *133*, 66–77.

Pardali, K., and Moustakas, A. (2007). Actions of TGF-beta as tumor suppressor and pro-metastatic factor in human cancer. Biochim. Biophys. Acta *1775*, 21–62.

Ponting, C.P., Oliver, P.L., and Reik, W. (2009). Evolution and functions of long noncoding RNAs. Cell *136*, 629–641.

Prensner, J.R., Iyer, M.K., Sahu, A., Asangani, I.A., Cao, Q., Patel, L., Vergara, I.A., Davicioni, E., Erho, N., Ghadessi, M., et al. (2013). The long noncoding RNA SChLAP1 promotes aggressive prostate cancer and antagonizes the SWI/SNF complex. Nat. Genet. *45*, 1392–1398.

Putoczki, T.L., Thiem, S., Loving, A., Busuttil, R.A., Wilson, N.J., Ziegler, P.K., Nguyen, P.M., Preaudet, A., Farid, R., Edwards, K.M., et al. (2013). Interleukin-11 is the dominant IL-6 family cytokine during gastrointestinal tumorigenesis and can be targeted therapeutically. Cancer Cell *24*, 257–271.

Salmena, L., Poliseno, L., Tay, Y., Kats, L., and Pandolfi, P.P. (2011). A ceRNA hypothesis: the Rosetta Stone of a hidden RNA language? Cell *146*, 353–358.

Subramanian, A., Tamayo, P., Mootha, V.K., Mukherjee, S., Ebert, B.L., Gillette, M.A., Paulovich, A., Pomeroy, S.L., Golub, T.R., Lander, E.S., and Mesirov, J.P. (2005). Gene set enrichment analysis: a knowledge-based approach for interpreting genome-wide expression profiles. Proc. Natl. Acad. Sci. USA *102*, 15545–15550.

Tao, Z.H., Wan, J.L., Zeng, L.Y., Xie, L., Sun, H.C., Qin, L.X., Wang, L., Zhou, J., Ren, Z.G., Li, Y.X., et al. (2013). miR-612 suppresses the invasive-metastatic cascade in hepatocellular carcinoma. J. Exp. Med. *210*, 789–803.

Tay, Y., Kats, L., Salmena, L., Weiss, D., Tan, S.M., Ala, U., Karreth, F., Poliseno, L., Provero, P., Di Cunto, F., et al. (2011). Coding-independent regulation of the tumor suppressor PTEN by competing endogenous mRNAs. Cell *147*, 344–357.

Thiery, J.P., Acloque, H., Huang, R.Y., and Nieto, M.A. (2009). Epithelial-mesenchymal transitions in development and disease. Cell *139*, 871–890.

Tsai, J.H., Donaher, J.L., Murphy, D.A., Chau, S., and Yang, J. (2012). Spatiotemporal regulation of epithelial-mesenchymal transition is essential for squamous cell carcinoma metastasis. Cancer Cell *22*, 725–736.

Yang, P., Li, Q.J., Feng, Y., Zhang, Y., Markowitz, G.J., Ning, S., Deng, Y., Zhao, J., Jiang, S., Yuan, Y., et al. (2012). TGF-β-miR-34a-CCL22 signaling-induced Treg cell recruitment promotes venous metastases of HBV-positive hepatocellular carcinoma. Cancer Cell *22*, 291–303.

Yang, L., Inokuchi, S., Roh, Y.S., Song, J., Loomba, R., Park, E.J., and Seki, E. (2013). Transforming growth factor-β signaling in hepatocytes promotes hepatic fibrosis and carcinogenesis in mice with hepatocyte-specific deletion of TAK1. Gastroenterology *144*, 1042–1054, e4.

Yoon, J.H., Abdelmohsen, K., Srikantan, S., Yang, X., Martindale, J.L., De, S., Huarte, M., Zhan, M., Becker, K.G., and Gorospe, M. (2012). LincRNA-p21 suppresses target mRNA translation. Mol. Cell *47*, 648–655.

Yuan, J.H., Yang, F., Chen, B.F., Lu, Z., Huo, X.S., Zhou, W.P., Wang, F., and Sun, S.H. (2011). The histone deacetylase 4/SP1/microrna-200a regulatory network contributes to aberrant histone acetylation in hepatocellular carcinoma. Hepatology *54*, 2025–2035.